Laser-induced alloying Au–Pd and Ag–Pd colloidal mixtures: the formation of dispersed Au/Pd and Ag/Pd nanoparticles†

Yu-Hung Chen, Yao-Hung Tseng and Chen-Sheng Yeh*

Department of Chemistry, National Cheng Kung University, Tainan, Taiwan, 701, R.O.C.
E-mail: csyeh@mail.ncku.edu.tw

Laser irradiation of colloidal mixtures consisting of Au–Pd and Ag–Pd were conducted to synthesize Au/Pd and Ag/Pd alloy nanoparticles. Compositional ratios of 1 : 1 and 2 : 1 were prepared in both the Au/Pd and Ag/Pd systems. The compositions, the particle sizes, and the morphology were measured as a function of the laser irradiation period in order to monitor the changes from the two-component mixtures into the alloy colloids. The average particle sizes of the 1 : 1 and 2 : 1 metal ratios were 3.9 ± 1.2 nm and 4.3 ± 1.1 nm, respectively, for Au/Pd and 7.3 ± 2.0 nm and 5.4 ± 2.0 nm, respectively, for Ag/Pd. However, Ag/Pd with a 2 : 1 ratio had difficult in forming dispersed spherical particles and the expected compositions. In addition to EDX analysis, X-ray diffraction measurements were carried out to confirm the formation of the alloy nanoparticles.

Introduction

Nanocomposites, *i.e.* alloy and core–shell particles, are highly valuable materials because of their composition-dependent optical and catalytic properties. Recently, we demonstrated a new methodology to fabricate Au/Ag alloy nanoparticles with ∼5 nm diameters using laser irradiation of gold and silver colloidal solutions.[1] El-Sayed *et al.*[2] and Koda *et al.*[3] suggested that the interaction between a laser beam and metal particles may lead to conformational changes *via* a melting process. We took advantage of this melting state, if present, and successfully alloyed a mixture containing two different kinds of metal particles under laser light irradiation. Interestingly, the interconnected network morphology, with its radial structures, was readily developed in the course of irradiation on the Au–Ag colloidal mixtures. This might suggest that the metals were at the melting stage. Thereafter, the particles switched to a spherical shape after the alloying process was complete.[1] In order to extend this technique to prepare other binary systems, it is also necessary to learn whether or not the formation of any composite particle shares a common transition process with the morphological transformation, as observed for the Au/Ag alloy. Au/Pd and Ag/Pd alloy colloids were chosen for these studies, where the compositions, the average diameters and the shapes of the prepared particles were measured as a function of the laser irradiation time.

In previous studies, both conventional chemical[4–6] and sonochemical[7–9] reductions were employed to prepare Au/Pd bimetallics, leading to a core(Au)/shell(Pd) structure. These methods generated core/shell Au/Pd diameters of less than 10 nm. A core–shell structural formation can be attributed to the differential redox potential in the metals. Murray *et al.*[10] successfully synthesized Au/Pd alloy clusters using a biphasic strategy. However, the shortcoming of their results was that the final compositional ratios of the resulting colloids could not be controlled simply by feeding the start metal salt ratios. Recently, Chen *et al.*[11] synthesized Au/Pd bimetallic particles using a reverse micelles methodology. In contrast to most

Au/Pd production as core–shell structures, alloyed Ag/Pd particles were prepared *via* chemical,[12,13] photochemical,[14] and radiolytic reductions.[15] In particular, Esumi *et al.*[14] formed dispersed and tiny Ag/Pd alloys with an average size of about 1−4 nm. However, the results from Vasan and Rao,[12] and Huang *et al.*[13] were the only data available in the literature that reported on prepared Ag/Pd compositions. A composite Pd/Ag with the core/shell property was developed by Henglein *et al.*[16] using, first, nucleated Pd particles, followed by reducing silver ions as the mantle.

Experimental

In this study Au and Ag nanoparticles were prepared in aqueous solution following the methods employed by Natan *et al.*[17] and Lee and Meisel,[18] respectively. The mean diameters of the prepared colloids were 13.7 ± 0.8 nm for Au and 16.8 ± 6.6 nm for Ag. Poly(vinyl alcohol) (PVA; MW, 22000) coated Pd particles were synthesized following the methodology of Thompson *et al.*[19] The prepared Pd colloids have small sizes, measured at 4.8 ± 1.8 nm. To prepare the Au–Pd or Ag–Pd colloidal mixtures in molar ratios of 1 : 1 and 2 : 1, it was assumed that 9.09×10^{-4} M of HAuCl$_4$, 2.1×10^{-4} M of AgNO$_3$, and 1.32×10^{-3} M of PdCl$_2$ were completely reduced into neutral metals. The total volume of the colloidal mixtures remained at 10 mL in the solution samples. That is 5.92 mL Au added to 4.08 mL Pd and 7.43 mL Au to 2.57 mL Pd constituted the molar ratios 1 : 1 (Au–Pd) and 2 : 1 (Au–Pd) mixtures, respectively. Using the same procedure, 8.65 mL of Ag and 1.35 mL of Pd colloids were mixed for a 1 : 1 (Ag–Pd) ratio and 9.28 mL of Ag and 0.72 mL of Pd colloids were used for a 2 : 1 (Ag–Pd) suspension. Triply distilled water was utilized throughout the experiments.

The resulting aqueous mixtures (10 mL) were placed in Pyrex vials. A Nd : YAG laser with a 5 ns pulse width operated at 10 Hz was used to produce the alloy nanoparticles. An unfocused 532 nm wavelength laser with a laser intensity of 2.45×10^2 mJ pulse^{-1} irradiated the colloidal mixtures during magnetic stirring. Irradiation was performed either by guiding the laser beam through the bottle opening or by a side-pump configuration to the vial containing the colloidal mixtures. The

laser beam diameter was controlled at 7.5 mm. The UV–vis absorption spectra of the colloidal suspensions were recorded using a Hewlett-Packard Model 8453 UV–vis spectrometer. Electron micrographs and EDX analysis using transmission electron microscopes (Hitachi FE-2000 and Zeiss 10c) were attained by placing a drop of the sample on a copper mesh coated with an amorphous carbon film, followed by evaporation of the solvent in a vacuum desiccator. The average diameters and size distributions were calculated using Sigma-Scan Pro 5.0 software for image analysis. XRD data were collected on a Rigaku D-Max IIIV diffractometer using Cu-Kα radiation (λ = 1.54056 Å) at 30 kV and 20 mA.

Results and discussion

Fig. 1 shows the UV–vis absorption development for the Au/Pd colloidal suspensions of the (a) 1 : 1 and (b) 2 : 1 molar ratios before and after laser irradiation. Prior to proceeding with irradiation, both colloidal mixtures (a and b) exhibited a prominent absorption maximum at 520 nm, attributed to the Au characteristic plasmon band. Note that Pd colloids do not have a distinct visible absorption band. It was found that the absorption band continuously decreased and showed no significant absorption peak as the irradiation time increased up to 40 min for the Au/Pd (1 : 1) ratio, as depicted in Fig. 1a. With increasing Au content, Fig. 1b shows that the UV–vis absorbance evolved an absorption band near 520 nm. The color of the suspensions varied from reddish-brown to dark brown for both Au/Pd ratios. Such changes in absorption and colloidal color might imply an change in colloidal property. As irradiation (>40 min) time increased no distinct change in the shape of the UV–vis absorbance and colloidal appearance occurred. For example, the TEM images showed that the dispersed spherical particles were attained at a 60 min exposure time and the average sizes were calculated as 4.6 ± 1.5 and 4.1 ± 1 nm for the 1 : 1 and 2 : 1 ratios, respectively, which are similar to the ones observed at an irradiation time of 40 min.

Fig. 2 shows the TEM images of the 1 : 1 molar ratio (Au/Pd) suspensions corresponding to (a) 0, (b) 20, and (c) 40 min laser
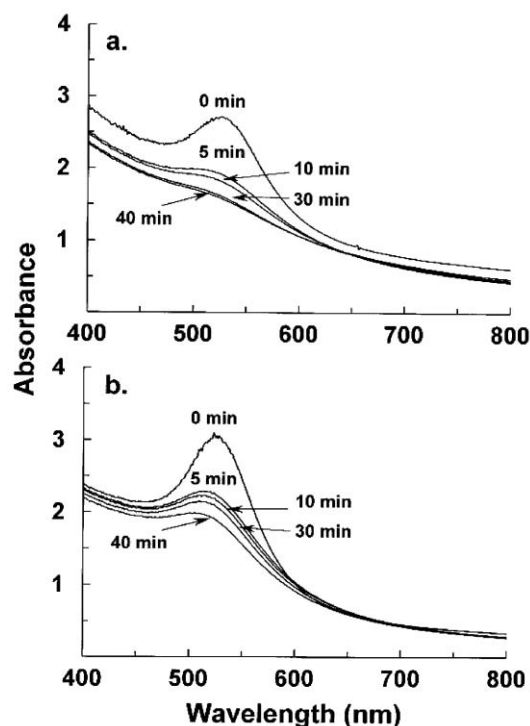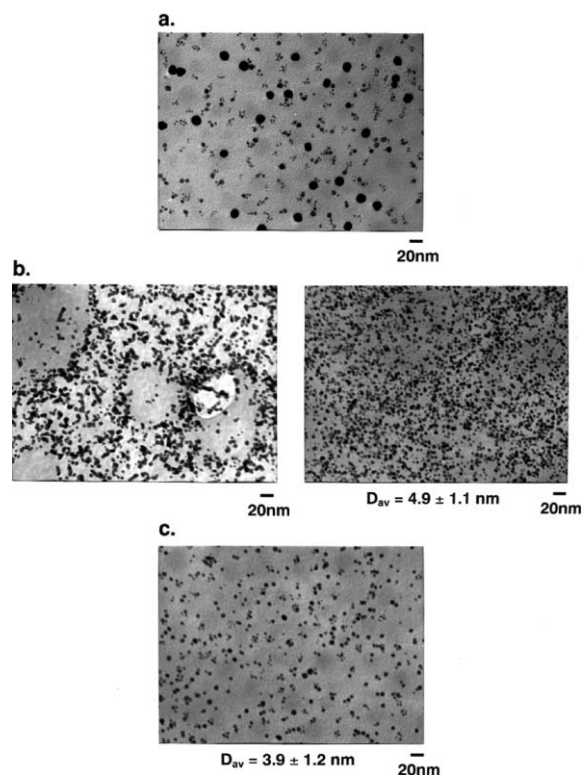

Fig. 2 TEM images of the 1 : 1 molar ratio (Au/Pd) colloidal suspensions after exposure to laser light for (a) 0 min, (b) 20 min, and (c) 40 min.

exposure times. In Fig. 2a, the prominent differentiation in particle sizes can be observed between Au and Pd, where the Au particles were revealed as large and dense contrast spheres while the much smaller ones were Pd. After irradiation for 20 min, the colloidal features altered significantly, as seen in Fig. 2b, with the appearance of two different structures: tiny spheres (the majority) and irregularly aggregated islands. By averaging the diameter of the spherical particles only, the mean size reduced to 4.9 ± 1.1 nm as compared with those in Fig. 2a. If the irradiation time increased to 40 min, the colloidal solutions were composed of dispersed spherical particles with a size of 3.9 ± 1.2 nm. In order to assess the overall picture of particle composition as a function of laser exposure time, EDX was utilized to measure discrete particles, which were chosen at random. As shown in Table 1, early irradiation gave rise to a large discrepancy in the mixing of the Au and Pd, and the particles seemed to become enriched in one component. If the laser exposure period was lengthened to 40 min, the final metal particle ratios tended to have a better agreement with the initial feeding molar ratios.

TEM measurements were applied to investigate the 2 : 1

Table 1 The atomic ratios (Au/Pd) analyzed using EDX in the selected particles, chosen at random

	Atomic ratio (Au/Pd) of the selected particles
Irradiation time (min) for molar ratio 1 : 1 of Au/Pd—	
10	60.3 : 39.7, 78.6 : 21.4, 87.7 : 12.3, 95.1 : 4.9
20	65.6 : 34.4, 71.6 : 28.4, 77.7 : 22.3
40	49.1 : 50.9, 52.8 : 47.2, 46.9 : 53.1, 44.3 : 55.7, 41.0 : 59.0, 39.0 : 61.0, 62.6 : 37.4, 70.0 : 30.0, 76.4 : 23.6
Molar ratio (Au/Pd); irradiation time/min—	
1 : 1; 40	49.1 : 50.9, 52.8 : 47.2, 46.9 : 53.1, 44.3 : 55.7, 41.0 : 59.0, 39.0 : 61.0, 62.6 : 37.4, 70.0 : 30.0, 76.4 : 23.6
2 : 1; 40	64.8 : 35.2, 64.5 : 35.5, 64.1 : 35.9, 69.3 : 30.7, 61.9 : 38.1, 75.5 : 24.5, 83.5 : 16.5

Fig. 1 Development of the UV–vis absorption spectra of the (a) 1 : 1 and (b) 2 : 1 molar ratios of Au/Pd colloidal suspensions as a function of the laser exposure time.

(Au/Pd) molar ratio as well (see ESI†). The alloy particles produced after 40 min exposure were chosen for EDX analysis, as seen in Table 1. Although particles with metal ratios (Au/Pd) larger than 2 cannot be excluded completely, the resulting colloidal compositions are essentially satisfactory with regard to the initial mixing proportions. Basically, no appreciable difference was observed in either 1:1 or 2:1 (Au/Pd) colloidal solutions with respect to their morphology and size distributions.

In this study, bimetallic Ag/Pd particles with ratios of 1:1 and 2:1 were also produced. Fig. 3a (1:1) and 3b (2:1) display the evolution of the absorption spectra associated with the laser exposure time. Due to a strong Ag plasmon band at 408 nm, its UV–vis absorbance at 0 min irradiation was truncated to fit in Fig. 3. After exposure to the laser light, the absorption intensities decreased significantly; in addition to the changes in the absorption contour. Interestingly, no apparent maximum absorption near the Ag surface plasmon band (408 nm) was seen with increasing Ag composition for Ag/Pd (2:1) when compared with the observed UV–vis spectra for the 2:1 Au/Pd ratio. These results might be because of the difficulty in forming a homogeneous compositional distribution for Ag/Pd (2:1), as mentioned later in the text. The colloidal color changed from yellowish-brown to brown. Fig. 4a–d display the corresponding TEM images shown for the curves of 0–55 min of Fig. 3a, respectively. At 0 min, the particles exhibited polydisperse features, as expected. Subsequent irradiation of the same solution for 10 min resulted in the formation of relatively monodisperse particles accompanied by the aggregated islands, showing the particles in close contact, as seen in Fig. 4b. Taking only the isolated spherical particles into account, the average size was measured as 6.1 ± 3.4 nm. Further irradiation of the solutions for 30 min and 55 min yielded the dispersed and well-separated spherical particles. Both 30 min and 55 min resulted in colloids with identical mean size and distribution. This may have been reflected in the UV–vis absorption curves at 30 and 55 min, which are almost the same in both shape and magnitude. Table 2 lists the changes in the compositions of the alloy particles (1:1, Ag/Pd) with respect to the irradiation time.
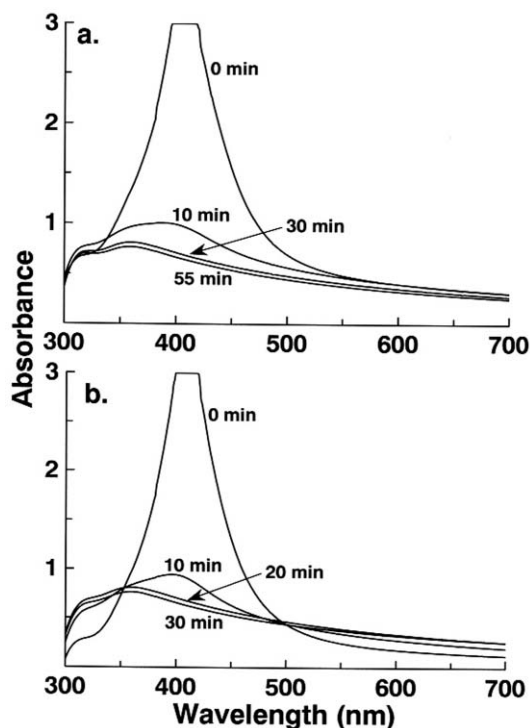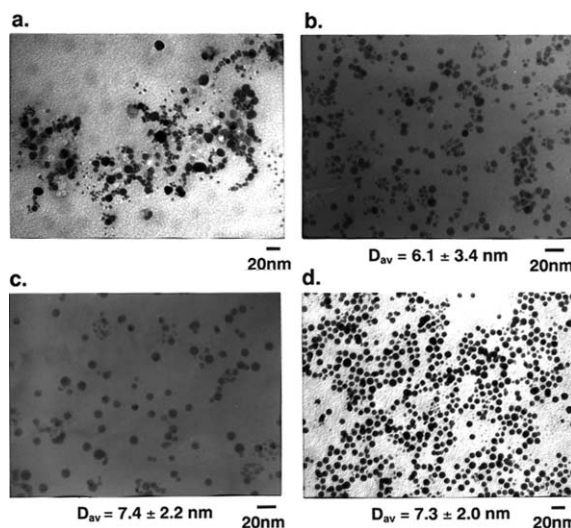

Fig. 4 TEM images of the Ag/Pd (1:1) colloids at various exposure times: (a) 0 min, (b) 10 min, (c) 30 min, and (d) 55 min.

The results indicate that both the 30 and 55 min irradiation stages lead to a better mixing ratio.

As seen in Fig. 3a and b, there is no distinct differentiation in the absorption spectra. However, the TEM images show the difficulty in forming the spherical bimetallic particles for the 2:1 (Ag/Pd) colloids (see ESI†). Significant irregular islands, some showing a cumulative aggregate with several particles chained together, appeared in each time period of laser irradiation. By consideration only the well-separated particles in the 20 min samples, the calculations gave a mean particle size of 5.4 ± 2.0 nm. The discrete spherical particles attained for the 2:1 (Ag/Pd) colloids were selected for EDX analysis. As shown in Table 2, the obtained spherical particles did not display a satisfactory composition for the Ag/Pd ratios near 2.

In addition to EDX analysis to obtain the particle compositions, XRD measurements were carried out to determine the formation of the alloy particles. Fig. 5 shows the XRD patterns of Au and Pd, and the Au/Pd (1:1 and 2:1) and Ag/Pd (1:1 and 2:1) particles. Broad peaks arose from the resulting Au/Pd and Ag/Pd powders located between the (111) reflections of the pure components (Au–Pd and Ag–Pd). This strongly suggested that the particles obtained were alloys. It is also clear that the diffraction peaks of the alloys exhibited a shift from pure Pd to pure Au and Ag as the coinage metal content increased.

As mentioned earlier, the accomplishment of these alloy experiments is based on the presence of the molten state in the nanoparticles. In previous studies on the interaction of a pulsed laser with nanoparticles, Koda et al.[3] irradiated spherical gold particles using a nanosecond laser with a wavelength of 532 nm and found a size reduction when the laser fluence was increased. Based on the correlation of the particle diameters

Fig. 3 Development of the UV–vis absorption spectra of the (a) 1:1 and (b) 2:1 molar ratio of Ag/Pd colloidal suspensions as a function of the laser exposure time.

Table 2 The atomic ratios (Ag/Pd) analyzed using EDX in the selected particles, chosen at random

| Atomic ratio (Ag/Pd) of the selected particles |
| --- |
| Irradiation time (min) for molar ratio 1:1 of Ag/Pd— |
| 10 44.9:55.1, 36.7:63.3, 34.4:65.6, 31.8:68.2, 30.0:70.0, 22.3:77.7, 97.5:2.5, 98.7:1.3 |
| 30 47.5:52.5, 43.6:56.4, 41.0:59.0, 40.0:60.0, 35.5:64.5, 34.7:65.3, 32.1:67.9, 98.3:1.7 |
| 55 48.3:51.7, 46.2:53.8, 57.2:42.8, 35.2:64.8, 59.6:40.4 |
| Molar ratio (Ag/Pd); irradiation time/min— |
| 1:1; 55 48.3:51.7, 46.2:53.8, 57.2:42.8, 35.2:64.8, 59.6:40.4 |
| 2:1; 20 67.0:33.0, 63.3:36.7, 62.3:32.7, 61.3:38.7, 71.2:28.8, 58.0:42.0, 57.8:42.2, 52.8:47.2, 51.4:48.6 |
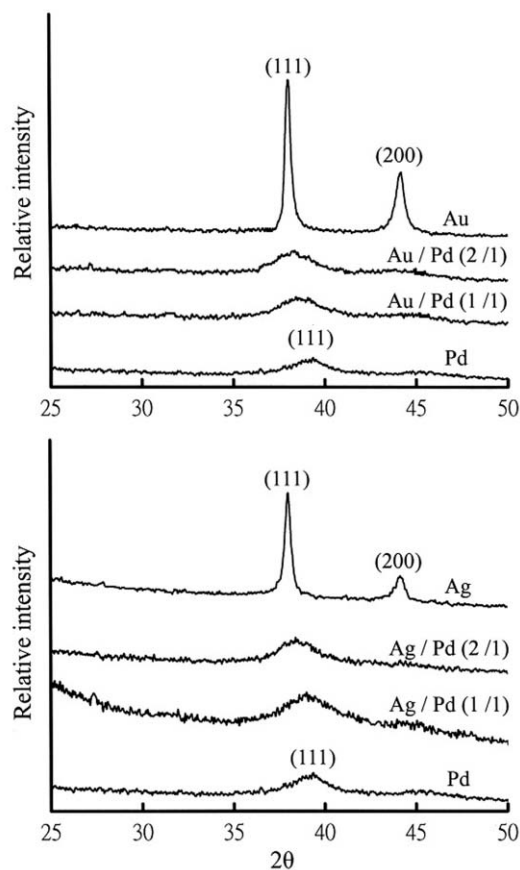
Fig. 5 XRD patterns of the individual Au, Ag and Pd particles as well as the Au/Pd and Ag/Pd alloy nanoparticles.

with the particle lattice temperatures, Koda *et al.*[3] interpreted the particle reshaping and fragmentation in terms of melting and vaporization processes. Furthermore, the studies on the conformational changes in Au nanorods by El-Sayed *et al.*[2] and the investigations into the laser-induced heating of $Au_{core}Ag_{shell}$ into an alloyed structure by Hartland *et al.*[20] examined the particle temperatures under femtosecond and picosecond excitation. In contrast to the conclusions of Koda *et al.*, El-Sayed *et al.*[2] thought that a thermal effect involving heating, melting and fragmentation of the hot lattice without vaporization behavior was responsible for the shape and size changes in nanoparticles exposed to nanosecond pulses. El-Sayed *et al.*[2] and Harland *et al.*[20] showed that the heat transfer from the lattice to the solvent cannot be ignored. The energy dissipated into the solvent in approximately 100–200 ps, which is much shorter than a nanosecond pulse.[20] At this stage, we are unable to study detailed alloying mechanisms due to a limited laser facility. However, it was found that the bimetallic compositions manifest a transition from one component enriched in the metal ratios consistent with the initial feeding proportions as the exposure time lengthened for the studies of the Au/Pd and Ag/Pd mixtures as a function of the laser irradiation time. This might imply that melting proceeds during the course of the laser irradiation.

Conclusions

These studies indicate that the laser-induced alloying methodology provides an efficient route to form a binary mixture at the atomic level, if both components are miscible in the bulk phase. The method of generating nanoparticles is different from laser ablation, which usually suffering from inhomogeneous sizes and significant aggregation, as the laser strategy produces dispersed particles with a narrow size distribution. Interestingly, we have seen no significant interconnected network, as found in the Au/Ag system, in the course of Au/Pd and Ag/Pd mixtures irradiation. Such a different occurrence remains to be resolved. The most significantly different observation between the Au/Pd and Ag/Pd systems is the degree of interconnection and the appearance of irregular features. For instance, it was found that the Ag/Pd colloids with a 2:1 ratio maintained the peculiar behavior of not forming uniform spherical particles and of not providing a satisfactory composition throughout the experiments.

References

1   Y. H. Chen and C. S. Yeh, *Chem. Commun.*, 2001, 371.
2   (*a*) S. Link, C. Burda, M. B. Mohamed, B. Nikoobakht and M. A. El-Sayed, *J. Phys. Chem. A*, 1999, **103**, 1165; (*b*) S. Link, C. Burda, B. Nikoobakht and M. A. El-Sayed, *J. Phys. Chem. B*, 2000, **104**, 6152.
3   A. Takami, H. Kurita and S. Koda, *J. Phys. Chem. B*, 1999, **103**, 1226.
4   G. Schmid, A. Lehnert, J.-O. Malm and J.-O. Bovin, *Angew. Chem., Int. Ed. Engl.*, 1991, **30**, 874.
5   H. Liu, G. Mao and S. Meng, *J. Mol. Catal.*, 1992, **74**, 275.
6   (*a*) N. Toshima, M. Harada, Y. Yamazaki and K. Asakura, *J. Phys. Chem.*, 1992, **96**, 9927; (*b*) M. Harada, K. Asakura and N. Toshima, *J. Phys. Chem.*, 1993, **97**, 5103.
7   Y. Mizukoshi, K. Okitsu, Y. Maeda, T. A. Yamamoto, R. Oshima and Y. Nagata, *J. Phys. Chem. B*, 1997, **101**, 7033.
8   K. Okitsu, M. Murakami, S. Tanabe and H. Matsumoto, *Chem. Lett.*, 2000, 1336.
9   R. Oshima, T. A. Yamamoto, Y. Mizukoshi, Y. Nagata and Y. Maeda, *Nanostruct. Mater.*, 1999, **12**, 111.
10 M. J. Hostetler, C. J. Zhong, B. K. H. Yen, J. Anderegg, S. M. Gross, N. D. Evans, M. Porter and R. W. Murray, *J. Am. Chem. Soc.*, 1998, **120**, 9396.
11 M. L. Wu, D. H. Chen and T. C. Huang, *Langmuir*, 2001, **17**, 3877.
12 H. N. Vasan and C. N. R. Rao, *J. Mater. Chem.*, 1995, **5**, 1755.
13 C. Y. Huang, H. J. Chiang, J. C. Huang and S. R. Sheen, *Nanostruct. Mater.*, 1998, **10**, 1393.
14 K. Esumi, M. Wakabayashi and K. Torigoe, *Colloids Surf. A*, 1996, **109**, 55.
15 H. Remita, J. Khatouri, M. Tréguer, J. Amblard and J. Belloni, *Z. Phys. D*, 1997, **40**, 127.
16 M. Michaelis, A. Henglein and P. Mulvaney, *J. Phys. Chem.*, 1994, **98**, 6212.
17 K. C. Grabar, R. G. Freeman, M. B. Hommer and M. J. Natan, *Anal. Chem.*, 1995, **67**, 735.
18 P. C. Lee and D. Meisel, *J. Phys. Chem.*, 1982, **86**, 3391.
19 S. Pathak, M. T. Greci, R. C. Kwong, K. Mercado, G. K. Surya Prakash, G. A. Olah and M. E. Thompson, *Chem. Mater.*, 2000, **12**, 1985.
20 J. H. Hodak, A. Henglein, M. Giersig and G. V. Hartland, *J. Phys. Chem. B*, 2000, **104**, 11708.